

SMITH-PURCELL RADIATION STUDIES TOWARDS A COMPACT HIGH-RESOLUTION LONGITUDINAL DIAGNOSTIC

B. Stacey^{*†}, W. Kuropka, T. Vinatier

Deutsches Elektronen-Synchrotron DESY, Hamburg, Germany

W. Hillert

Universität Hamburg, Hamburg, Germany

Abstract

A new longitudinal diagnostic has been proposed, the SPACEChip (Smith-Purcell ACcElerator Chip-based) diagnostic, which can infer information about the temporal profile of a particle bunch from the Smith-Purcell radiation spectrum generated when the bunch passes close to a dielectric grating. This is done using the bunch form factor after retrieving the phase information. A simulated dielectric grating has been excited by Floquet modes to investigate the angular distribution of the Smith-Purcell radiation. Progress on the SPACEChip experimental campaign at the ARES linac at DESY will be reported, along with the expected photon yield from the structure with the ARES operational parameters.

INTRODUCTION

When a charged particle bunch passes close to a periodic change in refractive index, i.e. a grating of dielectric material, it is induced to radiate via the Smith-Purcell radiation (SPR) mechanism [1] as demonstrated in Fig. 1. The emis-

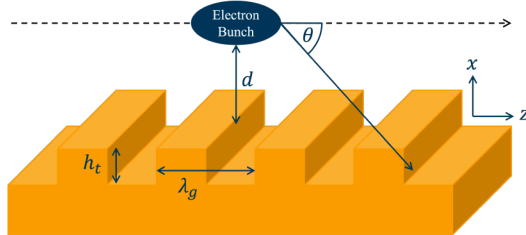


Figure 1: 3D model of SPR emission.

sion mechanism of SPR can be interpreted as the diffraction of the electron field [2]. SPR is spectrally dispersed and in-vacuum emission is governed by,

$$\frac{1}{\beta} - \cos(\theta) = \frac{m\lambda}{\lambda_g}, \quad (1)$$

where $\beta = v/c$, v is the velocity of the particle, c is the speed of light in a vacuum, θ is the angle of emission, m is the diffraction order, λ is the wavelength of the radiation, and λ_g is the period of the grating. For $m \neq 0$, Eq. (1) describes SPR of order m ; for $m = 0$, it describes Cherenkov radiation.

^{*} also at Universität Hamburg, Hamburg, Germany

[†] blaе.stacey@desy.de

The power radiated per angle is described by the angular distribution relation [2],

$$\frac{dP_m}{d\Omega} = \frac{eIm^2L}{2\lambda_g^2\epsilon_0} \frac{\sin^2\theta}{\left(\frac{1}{\beta} - \cos\theta\right)^3} |R_m|^2 e^{-\frac{d}{h_{int}}}, \quad (2)$$

where e is the elementary charge, I is the beam current, L is the length of the grating, ϵ_0 is the permeability of free space, and d is the impact parameter. $|R_m|^2$ is the radiation coefficient, which is discussed in detail for metallic rectangular and volume strip gratings in [3, 4]. h_{int} is the interaction length of the electron field virtual photons with the electron bunch,

$$h_{int} = \frac{\lambda\beta\gamma}{4\pi}, \quad (3)$$

where $\gamma = (1 - \beta^2)^{-1/2}$ is the Lorentz factor. Equation (2) assumes that the radiation is emitted in the x-z plane, as depicted in Fig. 1.

The use of SPR as a longitudinal bunch length diagnostic is not a new concept, however previous work has mostly involved using metal gratings [5–8]. Here, dielectric gratings are proposed, which can be produced with very high precision at low cost, due to advanced manufacturing techniques in the computer industry.

The reconstruction of the longitudinal bunch current profile is done through the use of the form factor. The radiated power consists of incoherent radiation, S_{inc} which is proportional to the horizontal charge profile of the bunch, and coherent radiation, S_{coh} , when the bunch length is shorter than λ_g , which is proportional to the entire three-dimensional current profile of the bunch. The total radiated power for a bunch of N_e electrons is,

$$\left(\frac{dP_m}{d\Omega}\right)_{N_e} = \left(\frac{dP_m}{d\Omega}\right)_1 (N_e S_{inc} + N_e^2 S_{coh}(\omega)), \quad (4)$$

where the form factor for the coherent radiation, S_{coh} , is given by,

$$S_{coh} = \left| \int_0^\infty X e^{-\frac{x}{\lambda_e}} dx \right|^2 \left| \int_{-\infty}^\infty Y e^{-ik_y y} dy \right|^2 \times \left| \int_{-\infty}^\infty T e^{-i\omega t} dt \right|^2, \quad (5)$$

where the charge distribution inside the bunch is assumed to be $q(x, y, t) = X(x)Y(y)T(t)$, λ_e is the evanescent wavelength and represents the coupling efficiency between the beam and the grating, k_y is the y component of the wave vector, and ω is the frequency of the radiation.

Table 1: Parameters of fused silica structure modelled in simulations and installed in UHV chamber at ARES linac.

Parameter	Value
Period	2.05 μm
Aperture	1 μm
Tooth Height	1750 μm
Length	1 mm

The characteristic impedance of the structure governs the expected photon yield for incoherent emission of SPR,

$$N_p = \sqrt{\frac{eN_e LZ}{h\lambda_g}} \quad (6)$$

where N_p is the number of photons, Z is the characteristic impedance, and h is Planck's constant.

In order to reconstruct the longitudinal current profile of the passing bunch, the phase information must be recovered. Although a review of the different phase reconstruction methods is beyond the scope of this work, the FROG technique [9] could be used. The relative phases could also be retrieved from the interference pattern of radiation emitted from different gratings.

SIMULATIONS

A single 2.05 μm period of a fused silica volume strip grating was modelled in CST and is described in Table 1. A Floquet excitation was provided by boundary conditions with a frequency equal to the period of the grating (146.2402 THz). Through the reciprocity principle, exciting the structure with a plane wave is comparable to observing the radiation emission directly. The resultant electric and magnetic fields were imported into a particle tracking solver, and the subsequent peak energy gain was used to calculate the characteristic impedance of the structure by analogy to circuit theory and Ohm's law. From a normal incident plane wave, a characteristic impedance for the structure was calculated to be 145 Ω , with a resolution determined by the simulation mesh. The incoming angle and frequency of the plane wave has been varied according to the relation in Eq. (1) to investigate the dependence of the characteristic impedance of the structure. A soft peak appears around -1° in Fig. 2, and for a frequency just above the data point equivalent to the period of the grating. It has been seen in Ref. [10] that position of the corresponding intensity peak can be tuned by optimising the geometry of the grating. Varying the tooth height, h_t , of the structure has a strong impact on the characteristic impedance, as presented in Fig. 3. This is in agreement with the oscillatory dependence observed in Ref. [11]. The tooth height can be tuned in the design stages to maximise the photon yield from a given structure. A single sided grating was also simulated with an electric boundary condition in place of the opposite grating to model a sheet of metal. The distance between the beam and the grating was varied, and Fig. 4 fits reasonably well to the exponential relation predicted by Eq. (2). The alignment of the particle beam

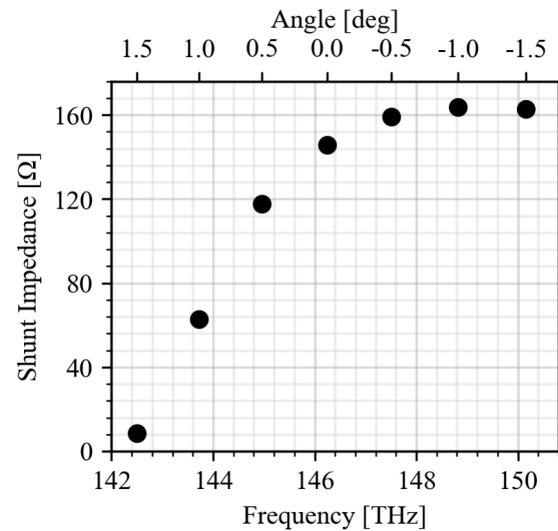


Figure 2: Characteristic impedance for incident plane waves with various angle and frequency combinations determined by Eq. (1).

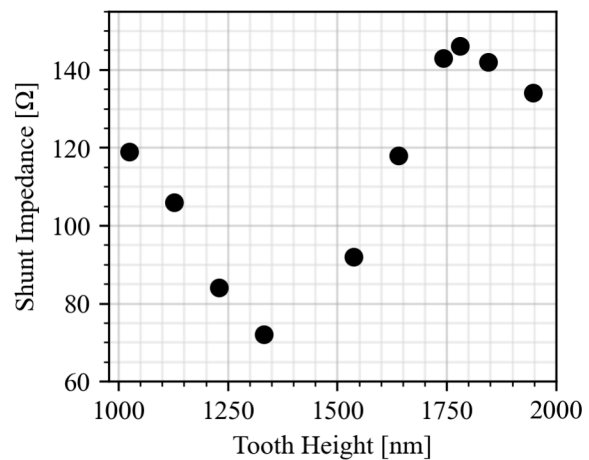


Figure 3: Characteristic impedance vs. tooth height.

through the aperture is no longer problematic for this set-up, although the characteristic impedance drops significantly for the single-sided grating case. This will reduce the potential SPR photon yield since it can be seen from Eq. (6) that $N_p \propto Z^{1/2}$ for incoherent SPR emission.

EXPERIMENTAL CAMPAIGN AT ARES

ARES (Accelerator Research Experiment at SINBAD) is a c. 45 m long S-band normal conducting linac dedicated to accelerator research and development [12]. A UHV (Ultra-High Vacuum) chamber is installed downstream of the linac section for DLA (Dielectric Laser Acceleration) experiments. It has a 6-dimensional translation stage with nanometer resolution for alignment optimisation of DLA structures. A quadrupole triplet before the chamber is able

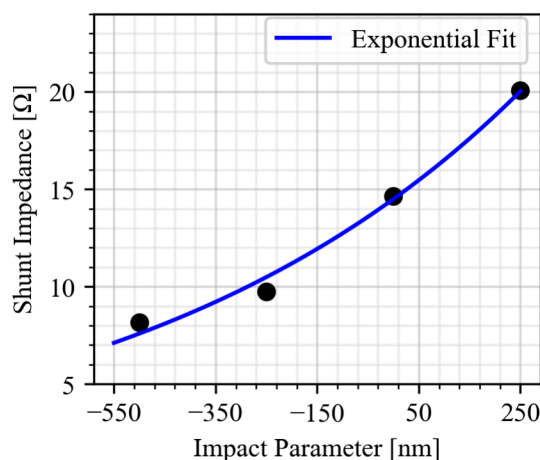


Figure 4: Characteristic impedance vs. impact parameter for a single-sided grating opposite an electric boundary condition.

to focus the beam to a transverse spot size on the order of $30\ \mu\text{m}$. A $2.05\ \mu\text{m}$ fused silica grating is currently installed

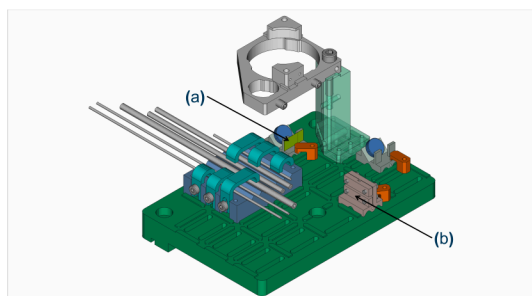


Figure 5: Image of baseplate on translation stage currently installed inside UHV chamber. (a) shows a YAG screen, for focusing the beam to a size comparable to the grating aperture, and (b) shows the holder for the fused silica grating. The grey cylinders on the left are for future longitudinal diagnostic experiments.

on the stage shown in Fig. 5. The parameters of this structure are shown in Table 1. A short 1pC 155MeV bunch can be focused to a small enough size that around 30% of the charge is transmitted through the structure. A velocity bunching working point has been established for the purpose of SPR experiments using this structure. Measurements of the bunch length have been performed using the PolariX TDS which is installed 20-meters downstream of the UHV chamber [13].

Radiation has been observed by a CCD camera that can image into the UHV chamber, and this is shown in Fig. 6. The camera is positioned roughly perpendicular to the radiation emission at $\theta = 90^\circ$. The acceptance angle of the camera has not yet been calibrated. It is likely that a large portion of this radiation is Cherenkov, generated from the untransmitted portion of the beam hitting the dielectric grat-

ing. This camera is not sensitive to the wavelength regime for coherent SPR, although small amounts of incoherent SPR are expected here. An InGaAs diode sensitive in the $2\ \mu\text{m}$ regime has been installed, but alignment was sensitive and overran the time constraints of this campaign. The ex-

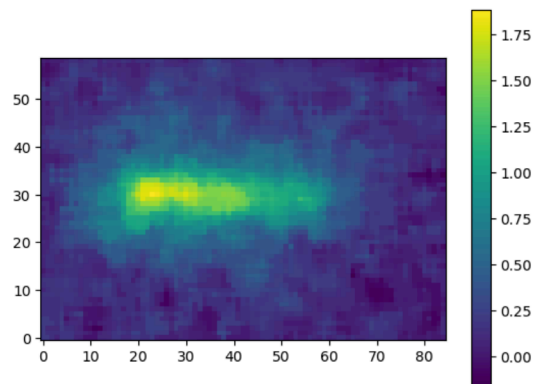


Figure 6: Cherenkov radiation and SPR emitted from dielectric grating imaged by CCD camera.

pected photon yield from this set-up can be calculated using Eq. (6) from the characteristic impedance of the structure described in Table 1 and the ARES beam parameters. Upon all emission being in the incoherent regime, the expected photon yield is 102 photons per grating period. By decreasing the bunch length below the period of the grating, it is expected that transition to the coherent-dominant regime can be observed, leading to an increased photon yield.

CONCLUSIONS

The SPR dependence on tooth height and impact parameter has been investigated here, and agreement has been found between prediction and observation. The expected photon yield per grating period has been calculated using the expected parameters at the ARES linac.

The availability of detection methods for THz radiation is the main limiting factor for using this concept to measure sub-femtosecond bunch lengths. Future work will include an in-air single-sided grating experiment at the end of the ARES linac and use as a 3D charge profile reconstruction in dispersive section of SwissFEL beamline. Radiation coefficients will be calculated according to Van der Berg's theory [3, 4].

REFERENCES

- [1] S. J. Smith and E. M. Purcell, "Visible Light from Localized Surface Charges Moving across a Grating", *Phys. Rev.*, vol. 92, no. 4, pp. 1069–1069, Nov. 1953. doi: 10.1103/physrev.92.1069
- [2] G. Toraldo di Francia, "On the theory of some Čerenkovian effects", *Il Nuovo Cimento*, vol. 16, no. 1, pp. 61–77, Apr. 1960. doi: 10.1007/bf02860231
- [3] G. Kube, "Calculation of Smith–Purcell radiation from a volume strip grating", *Nucl. Instrum. Methods Phys. Res.*,

- Sect. B*, vol. 227, no. 1–2, pp. 180–190, Jan. 2005.
doi:10.1016/j.nimb.2004.02.021
- [4] P. M. van den Berg and T. H. Tan, “Smith-Purcell radiation from a line charge moving parallel to a reflection grating with rectangular profile”, *J. Opt. Soc. Am. A*, vol. 64, no. 3, p. 325, Mar. 1974. doi:10.1364/josa.64.000325
- [5] P. Heil, K. Aulenbacher, C. Matejcek, S. Friederich, M. Bruker, and F. Fichtner, “Coherent Smith-Purcell radiation for minimally invasive bunch length measurement at the sub-picosecond time scale”, *Phys. Rev. Accel. Beams*, vol. 24, no. 4, Apr. 2021.
doi:10.1103/physrevaccelbeams.24.042803
- [6] S. E. Korbly, A. S. Kesar, R. J. Temkin, and J. H. Brownell, “Measurement of subpicosecond bunch lengths using coherent Smith-Purcell radiation”, *Phys. Rev. Spec. Top. Accel. Beams*, vol. 9, no. 2, p. 022802, Feb. 2006.
doi:10.1103/physrevstab.9.022802
- [7] H. L. Andrews *et al.*, “Reconstruction of the time profile of 20.35 GeV, subpicosecond long electron bunches by means of coherent Smith-Purcell radiation”, *Phys. Rev. Spec. Top. Accel. Beams*, vol. 17, no. 5, p. 052802, May 2014.
doi:10.1103/physrevstab.17.052802
- [8] V. Blackmore *et al.*, “First measurements of the longitudinal bunch profile of a 28.5 GeV beam using coherent Smith-Purcell radiation”, *Phys. Rev. Spec. Top. Accel. Beams*, vol. 12, no. 3, p. 032803, Mar. 2009.
doi:10.1103/physrevstab.12.032803
- [9] D. J. Kane and R. Trebino, “Single-shot measurement of the intensity and phase of an arbitrary ultrashort pulse by using frequency-resolved optical gating”, *Opt. Lett.*, vol. 18, no. 10, p. 823, May 1993. doi:10.1364/ol.18.000823
- [10] U. Haeusler, M. Seidling, P. Yousefi, and P. Hommelhoff, “Boosting the Efficiency of Smith–Purcell Radiators Using Nanophotonic Inverse Design”, *ACS Photonics*, vol. 9, no. 2, pp. 664–671, Jan. 2022.
doi:10.1021/acsp Photonics.1c01687
- [11] D. Konakhovych *et al.*, “Internal Smith-Purcell radiation and its interplay with Cherenkov diffraction radiation in silicon – a combined time and frequency domain numerical study”, May 2021. doi:10.48550/arXiv.2105.07682
- [12] F. Burkart *et al.*, “The ARES Linac at DESY”, in *Proc. LINAC’22*, Liverpool, UK, Aug.-Sep. 2022, pp. 691–694.
doi:10.18429/JACoW-LINAC2022-THP0J001
- [13] S. Jaster-Merz *et al.*, “5D tomographic phase-space reconstruction of particle bunches”, *Phys. Rev. Accel. Beams*, vol. 27, no. 7, Jul. 2024.
doi:10.1103/physrevaccelbeams.27.072801